



Quantitative data analysis of ESAR data

N. Phruksahiran and M. Chandra

Professorship of Microwave Engineering and Electromagnetic Theory, Chemnitz University of Technology, Germany

Correspondence to: N. Phruksahiran (narathep.phruksahiran@s2009.tu-chemnitz.de)

Abstract. A synthetic aperture radar (SAR) data processing uses the backscattered electromagnetic wave to map radar reflectivity of the ground surface. The polarization property in radar remote sensing was used successfully in many applications, especially in target decomposition. This paper presents a case study to the experiments which are performed on ESAR L-Band full polarized data sets from German Aerospace Center (DLR) to demonstrate the potential of coherent target decomposition and the possibility of using the weather radar measurement parameter, such as the differential reflectivity and the linear depolarization ratio to obtain the quantitative information of the ground surface. The raw data of ESAR has been processed by the SAR simulator developed using MATLAB program code with Range-Doppler algorithm.

1 Introduction

Nowadays, SAR Technology has been continuously developed by many researchers. Therefore, many benefits of polarimetric SAR (PolSAR) by using the physically properties of scattering mechanisms in the polarization signature was found. This leads to many theories and applications in the field of target decomposition. The polarimetric decomposition theorems can be classified into coherent and incoherent target decompositions which have each different advantage. The coherency decomposition deal with the scattering matrix, the incoherent decomposition is based on the coherency or covariance matrices. In addition to the full polarimetric SAR systems that transmit two orthogonal polarizations and record both received polarization, i.e., (hh, hv, vh, vv), where h and v denote the horizontal and vertical polarizations, respectively, there is the so-called dual-pol SAR modes, that consider only two linear polarizations, i.e., (hh,hv), (vh,vv) and (hh,vv). Another parameter of interest are the differential reflectivity (Z_{dr}) and the linear depolarization ratio (L_{dr}),

that can be used to process the weather radar data to obtain the qualitative measurements.

In this paper, SAR simulator was developed by using MATLAB program in order to process the experimental data from DLR with Range-Doppler processing algorithm. The processed full-polarized data was used to investigate the some potential of the coherent decompositions in SAR polarimetry.

This paper is organized as follows. In Sect. 2 we introduce the basics of the target decomposition, and in Sect. 3 we explain the experimental data and the data processing. In Sect. 4, the simulation results are presented. Finally, Sect. 5 provides the conclusions.

2 Basics

In general, the radar image of SAR system presents the magnitude of each pixel which can be scaled to show the depth of the image, so that we can interpret it like the optical image. The visual analysis needs the correct perception of the observer to identify the targets on the ground. The target decomposition theorems are developed based on the wave polarization basis to aim at providing such an interpretation.

The main categories of decompositions and parameter considered in this paper are the following: Pauli decomposition, differential reflectivity and linear depolarization ratio.

2.1 Pauli decomposition

Pauli decomposition is the most common known decomposition and expresses the scattering matrix $[S]$ as the complex sum of the Pauli matrices which can be written as shown by Lee (2009):

$$[S] = \begin{bmatrix} S_{hh} & S_{hv} \\ S_{vh} & S_{vv} \end{bmatrix} \quad (1)$$

$$= \frac{a}{\sqrt{2}} \begin{bmatrix} 1 & 0 \\ 0 & 1 \end{bmatrix} + \frac{b}{\sqrt{2}} \begin{bmatrix} 1 & 0 \\ 0 & -1 \end{bmatrix} + \frac{c}{\sqrt{2}} \begin{bmatrix} 0 & 1 \\ 1 & 0 \end{bmatrix} + \frac{d}{\sqrt{2}} \begin{bmatrix} 0 & -j \\ j & 0 \end{bmatrix} \quad (2)$$

The parameter a, b, c and d are complex quantities representing, respectively, single or odd-bounce scattering, double or even-bounce scattering, 45° rotated double-bounce scattering, and the anti-symmetric components of the scattering matrix, and are given by:

$$a = \frac{S_{hh} + S_{vv}}{\sqrt{2}} \quad (3)$$

$$b = \frac{S_{hh} - S_{vv}}{\sqrt{2}} \quad (4)$$

$$c = \frac{S_{hv} + S_{vh}}{\sqrt{2}} \quad (5)$$

$$d = j \frac{S_{hv} - S_{vh}}{\sqrt{2}}. \quad (6)$$

In the case of the monostatic radar operation, it is assumed that $S_{hv} = S_{vh}$, and the Span value is given by:

$$\text{Span} = |S_{hh}|^2 + 2|S_{hv}|^2 + |S_{vv}|^2 = |a|^2 + |b|^2 + |c|^2. \quad (7)$$

The color-coded representation with the basic colors (red, blue, green) can be used to recreate the image corresponding to the color-coded of each complex quantity.

2.2 Differential reflectivity and linear depolarization ratio

The differential reflectivity (Z_{dr}) and the linear depolarization ratio (L_{dr}) are commonly used in weather radar measurements. At the weather radar, the target volume is taken for analysis. The SAR system receives the reflected signals of ground targets and processes the data to the final image that represents the reflection properties of the ground.

The differential reflectivity Z_{dr} can be calculated in dB as the ratio of the reflectivity in horizontal polarization S_{hh} and the reflectivity in vertical polarization S_{vv} by the following equation as shown by Yanovsky (2000):

$$Z_{dr} = 10 \cdot \log_{10} \frac{S_{hh}}{S_{vv}}. \quad (8)$$

The important information from the Z_{dr} value depends on the target structure. If Z_{dr} is closely zero, the structure is sphere. The structure has the more length in horizontal axis when the Z_{dr} value is more than zero. Adversely, the Z_{dr} value is less than zero then, the structure has the more length in vertical axis.

The linear depolarization ratio L_{dr} is one of the interesting ratios from measurement and is the fraction of refractivity



Fig. 1. Google Earth image of the test area.

between the co- and cross-polar radar signal channels by the following equation:

$$L_{dr} = 10 \cdot \log_{10} \frac{S_{vh}}{S_{hh}}. \quad (9)$$

3 Experimental data and data processing

The experimental L-Band full polarized of OPAIR Test Site Area of Germany data set, which was used in this paper, is from the airborne ESAR flown by the German Aerospace Center (DLR), obtained on 20 February 2003. The terrain, as shown in Fig. 1, is a mixture of the flat surfaces, trees and buildings.

There are numerous SAR simulators for development of a radar system and radar processing. In this paper the range Doppler algorithm have been chosen to process the SAR raw data from ESAR.

The overview of the ESAR data signal processing with range Doppler algorithm and the target decomposition is shown in Fig. 2. The SAR simulator program was developed to read the binary raw data and to convert it to the two dimension SAR matrices data in range and azimuth direction for the following data processing as shown by Cumming (2005).

In each step of the SAR data processing, the required system parameters, the frequency, the bandwidth, the pulse length and the geometry, have been added into the simulation program. The signal processing in this paper with range Doppler algorithm in frequency domain takes place in order of range compression, range migration correction and azimuth compression. The range compression is performed when the data are in the azimuth time domain with a fast convolution by using the matched filter function in the range direction. The range migration correction is performed in the range Doppler domain to straighten out the target trajectories at the same range into on single trajectory that run parallel

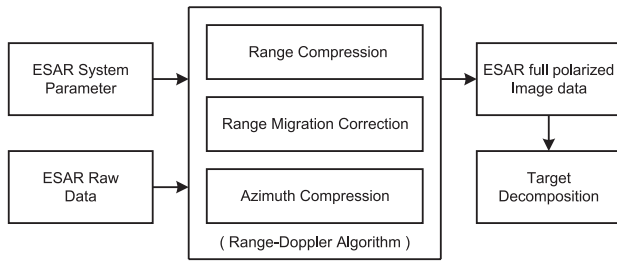


Fig. 2. Functional block diagram of ESAR signal processing with range Doppler algorithm and target decomposition.



Fig. 3. Image data of hh-polarization channel from ESAR (DLR).

to the azimuth frequency axis. The azimuth compression is performed by using the matched filter function at each range gate. Then the processed data of the respective polarization channels are used for the purpose of target decomposition.

4 Results

This section presents the simulation results for the purpose of the alternative or supplement information of polarimetric SAR data to the existing target decomposition methods.

4.1 Image data

After digital signal processing, the four polarized data sets have been created in hh, hv, vh and hv polarization. The Image data can be shown with gray scale by using the difference of signal intensity from the target or the surface of interest. The signal intensity depends on the scattering properties of each target structure according to the polarization state of the SAR operation. In this paper, we used the Range-Doppler algorithm to process each SAR data channel, i.e., hh, hv, vh and vv, with the same system parameter and data processing in frequency domain.



Fig. 4. Pauli decomposition, the image is colored by blue for $|a|^2$; red for $|b|^2$; green for $|c|^2$.

Figure 3 presents the image data of ESAR data set in hh polarization after the signal processing with Range-Doppler algorithm with sub-aperture length in azimuth direction and without the multi-look processing to reduce the speckle noise which arises in SAR because the relative phase of individual scatters. So that we can get and use the original image data set to test the target decomposition method and quantitative parameter of radar image as following.

4.2 Pauli decomposition

In general, the Pauli decomposition provides a tool for image classification that has been well known for decades in radar remote sensing communities. The three component of the Pauli composition are represented with color-coded blue, $|a|^2$; red, $|b|^2$ and green, $|c|^2$, respectively. Figure 4 presents the corresponding color-coded Pauli reconstructed image.

If we compare Fig. 1 with Fig. 4, we can realize the Pauli signatures of each part on the test area. The area on the right above is the residential area with many houses, which have the structure of dihedral, the red color dominates. The runway and street areas are presented by dark tone. It is clear to see that the forest area is in green. The areas in which the scattering mechanisms are simultaneously presented are shown with white. The different colors show that each polarization provides other information.

4.3 Differential reflectivity and linear depolarization ratio

In order to provide alternative verification of the differential reflectivity and linear depolarization ratio in SAR target decomposition method, the simulated images are provided in Fig. 5 and Fig. 6 for differential reflectivity and linear depolarization ratio, respectively.

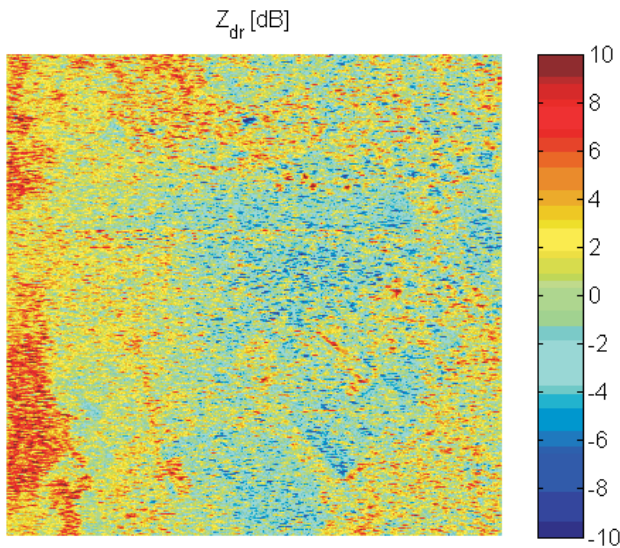


Fig. 5. Simulation results of Z_{dr} of test site area in dB.

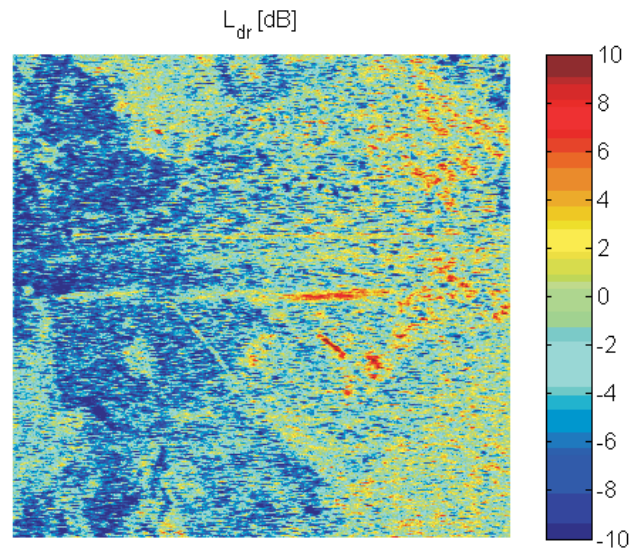


Fig. 6. Simulation results of L_{dr} of test site area in dB.

4.3.1 Z_{dr} values

Figure 5 presents the simulation results of differential reflectivity by using the reflectivity difference between hh- and vv polarization SAR operation. The values are shown in dB with the value range $[-10, 10]$.

By using the color-coded according to the Z_{dr} values, one can see that there are different shades of each area on the image. When considered as a whole, it can be seen that the smooth area has the Z_{dr} values less than zero, the blue color dominates. The another area which consists of a building or area of forest has the Z_{dr} values more than zero, the red color dominates. In the area of forest and building, there is not much of difference from each other. By using the differential reflectivity, we can see and image the contour of the ground structure and it can be separated the flat area from the area with forest and building.

4.3.2 L_{dr} values

Figure 6 presents the simulation results of linear depolarization ratio by using the reflectivity difference between vh- and hh polarization SAR operation. The values are shown in dB with the value range $[-10, 10]$.

The values of linear depolarization ratio as shown in Fig. 6 have the uneven distribution. But one can indicate that the values of L_{dr} are less than zero for the smooth area and the values of L_{dr} are more than zero for the area with buildings.

4.3.3 Applied Z_{dr} values

In Fig. 5, we have defined a continuous change of color-coded of the differential reflectivity values to compare the values obtained from the experiments, so that we can see the approximately difference between each type of surface.

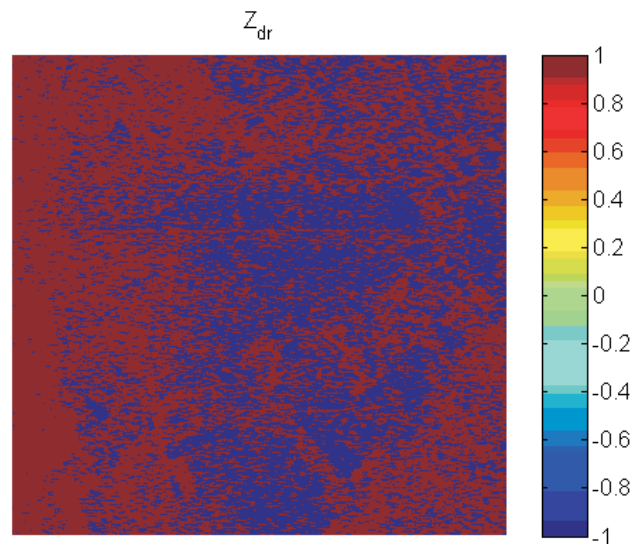


Fig. 7. Applied Z_{dr} values with -1 and 1 .

Figure 7 presents the simulation results of differential reflectivity by using the reflectivity difference between hh- and vv polarization SAR operation. The values are shown with -1 and 1 for the Z_{dr} values which are less than zero and the Z_{dr} values which are equal or more than zero, respectively.

The applied adjustment of the display color-coded makes it possible to see the lines and the contour of the surface character. Although it cannot be stated clearly that the surface looks like or consists of any object type. The target decomposition by using the applied Z_{dr} values can provide information correctly that the ground surface is flat or that the buildings or the forests are in the area. In this paper, it can be determined that if the surface is smooth, the value of the

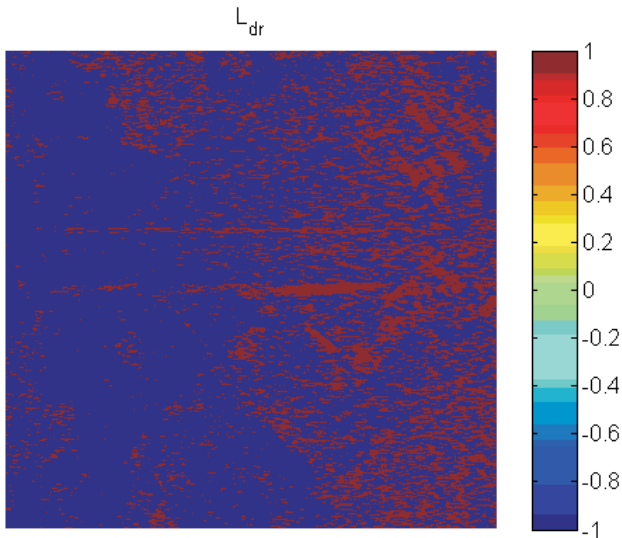


Fig. 8. Applied L_{dr} values with -1 and 1 .

variable Z_{dr} are equals to -1 and if the surface is not smooth, the value of the variable Z_{dr} are equals to 1 .

4.3.4 Applied L_{dr} values

The same approach to the display the applied Z_{dr} values in Fig. 7 has been used to present the simulation results of the linear depolarization ratio from the Fig. 6, so that the values in the Fig. 8 are shown with -1 and 1 for the L_{dr} values which are less than zero and the L_{dr} values which are equal or more than zero, respectively.

The benefit of this approach is the values of L_{dr} in the area with large buildings. By comparing the location of the building in Fig. 1 one can see the border of the building in Fig. 8 at the same location as well.

4.4 Comparison of applied Z_{dr} values and applied L_{dr} values

By comparing the values of the applied differential reflectivity in Fig. 7 and the applied linear depolarization ratio in Fig. 8 at each area, it can be divided in four cases as following:

1. $+Z_{dr}$ and $+L_{dr}$: the areas that may have a positive Z_{dr} values and positive L_{dr} values are larger building.
2. $+Z_{dr}$ and $-L_{dr}$: in the vicinity of the houses or villages with a characteristic dihedral structure, the Z_{dr} may have a positive values but the L_{dr} may have negative values.

3. $-Z_{dr}$ and $+L_{dr}$: in this case, it is not possible to determine exactly what are the surface characteristics and the kind of target.

4. $-Z_{dr}$ and $-L_{dr}$: the simulation results also indicate that the flat area and fields may have the negative values of Z_{dr} and L_{dr} .

5 Conclusions

In the first part of this paper, we have provided a short review of Pauli decomposition, differential reflectivity and linear depolarization ratio. The SAR simulator was developed to process the polarimetric raw data set of ESAR from DLR with range Doppler algorithm. The findings indicate that some parameter which was used to evaluate weather data set such as differential reflectivity and linear depolarization ratio can be used for the decomposition purpose in SAR radar remote sensing and they are considered as a useful addition to the decomposition theorems. Since the simulation results are obtained with only one polarimetric test data set, the interpretation and the conclusion have particular limitation. Further work will also include the development of improved simulation method for a better interpretation of the various target decompositions, in particular the alternative measurement parameter, e.g., the differential reflectivity and the linear depolarization, as an additional feature of the target decomposition method in SAR image data.

Acknowledgements. The authors would like to thank Alberto Moraira of DLR, Germany, for providing the full polarimetric ESAR data set which was used in EU project AMPER.

References

Cumming, I. G. and Wong, F. H.: Digital Processing of Synthetic Aperture Radar Data Algorithms and Implementation, Artech House, Norwood, 2005.

Klausing, H. and Holpp, W.: Radar mit realer und synthetischer Apertur Konzeption und Realisierung, Oldenbourg, Muenchen, 2000.

Lee, J. S. and Pottier, E.: Polarimetric Radar Imaging from Basics to Applications, CRC Press, Boca Raton, 2009.

Yanovsky, F. J., Russchenberg, H. W. J., Ligthart, L. P., and Fomichev, V. S.: Microwave Doppler-polarimetric technique for study of turbulence in precipitation, in: Proceedings of IGARSS 2000, Honolulu Hawaii, USA, 24–28 July 2000, 2296–2298, 2000.